Physica E 41 (2009) 533–536

Contents lists available at ScienceDirect

Physica E

journal homepage: www.elsevier.com/locate/physe

Synthesis of one-dimensional SnO_2 nanorods via a hydrothermal technique

O. Lupan [a,b,*], L. Chow [a], G. Chai [c], H. Heinrich [a,d,e], S. Park [a], A. Schulte [a]

[a] Department of Physics, University of Central Florida, PO Box 162385, Orlando, FL 32816-2385, USA
[b] Department of Microelectronics and Semiconductor Devices, Technical University of Moldova, 168 Stefan cel Mare Blvd., Chisinau MD-2004, Republic of Moldova
[c] Apollo Technologies, Inc. 205 Waymont Court, S111, Lake Mary, FL 32746, USA
[d] Advanced Materials Processing and Analysis Center, University of Central Florida, Orlando, FL 32816, USA
[e] Department of Mechanical, Materials, Aerospace Engineering, University of Central Florida, Orlando, FL 32816, USA

ARTICLE INFO

Article history:
Received 19 August 2008
Received in revised form
7 October 2008
Accepted 8 October 2008
Available online 17 October 2008

PACS:
81.10.Dn
61.46.−w
61.46.Km
68.37.Lp
78.30.Fs

Keywords:
SnO_2 nanorod
Crystal structure
Semiconductors
Hydrothermal synthesis
Raman spectra

ABSTRACT

We have developed a simple solution process to synthesize tin oxide nanorods. The influence of precursors and the reaction temperature on the morphology of SnO_2 is investigated. SnO_2 nanorods are characterized by X-ray diffraction (XRD), transmission electron microscopy (TEM), scanning electron microscopy (SEM), and Raman spectroscopy. The as-grown SnO_2 nanorods are uniform in size with a radius of 50–100 nm and length of 1–2 μm. The nanorods grow direction is parallel to the [1 0 1] direction. Possible growth mechanism of SnO_2 nanorods is discussed.

1. Introduction

Controlled synthesis of nanostructures is an important step for the manufacturing of nanodevices. Performance of semiconductor nanodevices may depend on their morphology. Recently, one-dimensional (1D) materials have attracted great interest due to their potential applications as interconnects and functional components [1–5]. 1D oxide nanostructures showed interesting properties, chemical and thermal stability, diverse functionalities, high durability, owing to their high degree of crystallinity [3], and emerge as nanoscale building blocks for electronic and optoelectronic devices [4,5]. At the same time, the interest in developing parts per billion (ppb)-level gas sensors requires new approaches and new nanomaterials. One of the most important sensor materials is tin oxide (SnO_2), which is a low-cost, large-bandgap (3.6 eV, at 300 K), and n-type semiconductor [6]. SnO_2's properties are greatly affected by the size and morphology, which define their further applications. Thus, designing SnO_2 1D nanorods and nanoarchitectures with well-defined morphologies is of importance for fundamental research and high-tech applications.

Fabrication of SnO_2 nanorods has been accomplished using several vapor deposition techniques, such as rapid oxidation [7], chemical vapor deposition (CVD) [8], and thermal evaporation [9]. Peng et al. [10] have recently reported a hydrothermal synthesis of SnO_2 nanorods. However, organic reagents such as hexanol and sodium dodecylsulfate used in the synthesis of SnO_2 nanorods can lead to undesirable impact on human health and on the environment [6]. Zhang et al. [11] also reported a low-temperature fabrication (at 200 °C for 18 h) via a hydrothermal process of crystalline SnO_2 nanorods. Vayssieres et al. [12] reported SnO_2 nanorods arrays grown on F-SnO_2 glass substrates by aqueous thermohydrolysis at 95 °C.

In this work we report a simple, one-step low-temperature aqueous synthesis of SnO_2 1D nanorods without the need of templates or surfactants.

2. Experimental details

The SnO_2 nanorods were synthesized via a hydrothermal method, which is similar to the method used in SnO_2 microcubes

* Corresponding author at: Department of Physics, University of Central Florida, 4000 Central Florida Blvd PO Box 162385, Orlando, FL 32816-2385, USA.
Tel.: +1 407 823 5217.
E-mail address: lupan@physics.ucf.edu (O. Lupan).

1386-9477/$ - see front matter © 2008 Elsevier B.V. All rights reserved.
doi:10.1016/j.physe.2008.10.001

[13] and ZnO nanorods synthesis [14]. In a typical synthesis, 50 ml $SnCl_4$ aqueous solution (in deionized (DI) water resistivity—18.2 MΩ cm) in the presence of 1 ml of HCl (37%) and NH_4OH (29.5%) (Purchased from Fisher Scientific) solution was mixed and stirred for 5 min. The mixing solution was then transferred to a reactor [14]. It was heated to 95 °C and kept for 15 min. Then the system was allowed to cool to 40 °C naturally. A silicon substrate were cleaned as previously described [15] and placed inside the reactor.

The structural properties of SnO_2 nanorods were determined by X-ray diffraction (XRD) (Rigaku 'D/Max-b(R)' X-ray diffractometer with CuKα radiation and a normal θ–2θ scan) [14]. The morphologies of the SnO_2 nanorods were studied by a scanning electron microscopy (SEM). Transmission electron microscopy (TEM) observation of the samples was performed with a FEI Tecnai F30 TEM operated at an accelerating voltage of 300 kV. For the TEM observation, the products were collected on a holey carbon grid. Micro-Raman measurements were performed at room temperature on a Horiba Jobin Yvon LabRam IR system at a spatial resolution of 2 μm. Raman scattering was excited with the 633 nm line of a He–Ne laser with output power <4 mW at the sample.

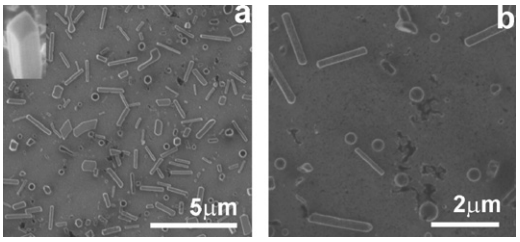

Fig. 1. SEMs of the SnO_2 nanorods hydrothermally grown (a) and closer view (b). Inset shows a magnified image of cross section of the SnO_2 nanorods.

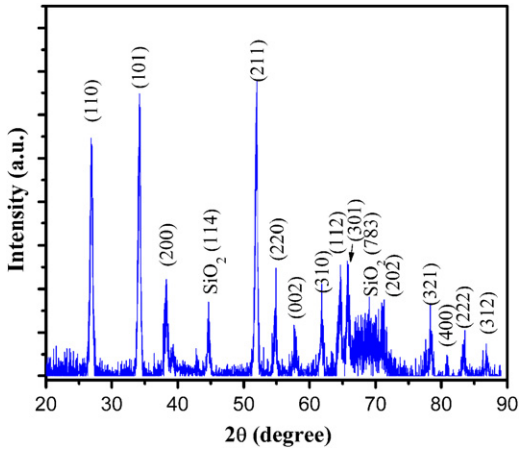

Fig. 2. The XRD pattern of the SnO_2 nanorods grown via the hydrothermal method.

3. Results and discussion

Fig. 1 shows the SEM images of the as-grown products synthesized on SiO_2/Si substrates. The products consist of nanorods as well as nanoparticles. The diameters of SnO_2 nanorods are in the range of 100–150 nm with lengths of the order of 1–2 μm. The end planes of the nanorods are tetragonal (see inset Fig. 1a).

The morphology of nanorods is found to be dependent on the synthesis conditions. The dimensions and aspect ratio are a function of growth time, temperature and Sn^+/OH^- ratio in solution.

The XRD pattern of SnO_2 nanorods is shown in Fig. 2. There are peaks with 2θ values of 26.97°, 34.34°, 38.26°, 52.01°, 54.90°, 71.28°, and 78.40°, corresponding to SnO_2 tetragonal rutile crystal planes of (1 1 0), (1 0 1), (2 0 0), (2 1 1), (2 2 0), (2 0 2), and (3 2 1), respectively. Observed peaks can be indexed to the rutile-structured SnO_2 with lattice constants $a = b = 0.4738$ nm and $c = 0.3185$ nm, (JCPDS-PDF# 021-1250)(ICSD data) [16]. Two SiO_2 peaks were observed at 44.70°, a reflection from (1 1 4), and at 68.87°, a reflection from (7 8 3) planes. The XRD pattern demonstrates that the products grown under hydrothermal conditions are SnO_2 of good crystallinity, with the obtained diffraction peaks, broadened by the small diameter of the nanorods.

A TEM image of a single SnO_2 nanorod with a diameter of about 100 nm is shown in Fig. 3. Further characterization was performed using HRTEM. Fig. 3b shows an HRTEM image of a nanorod. The corresponding selected-area electron diffraction (SAED) pattern taken from a section of the nanorod shown in Fig. 3c can be indexed to the tetragonal cell with lattice constants of $a = 0.474$ nm and $c = 0.318$ nm, in agreement with the XRD result. The SAED pattern also confirms that the nanorod is a single crystalline rutile SnO_2 with preferential growth direction along the [1 0 1] direction, confirming the XRD analysis.

Raman spectra are sensitive to crystallinity, defects and structural disorder in nanoarchitectures. Therefore, the vibrational properties of SnO_2 nanorods were studied by Raman spectroscopy.

Fig. 4 shows Raman spectra in Stokes frequency range (200 cm^{-1}–850 cm^{-1}) of the products annealed for 1 h at 370 °C. There are Raman peaks at 475, 632, and 774 cm^{-1} in the Raman spectrum which are in agreement with those of a rutile SnO_2

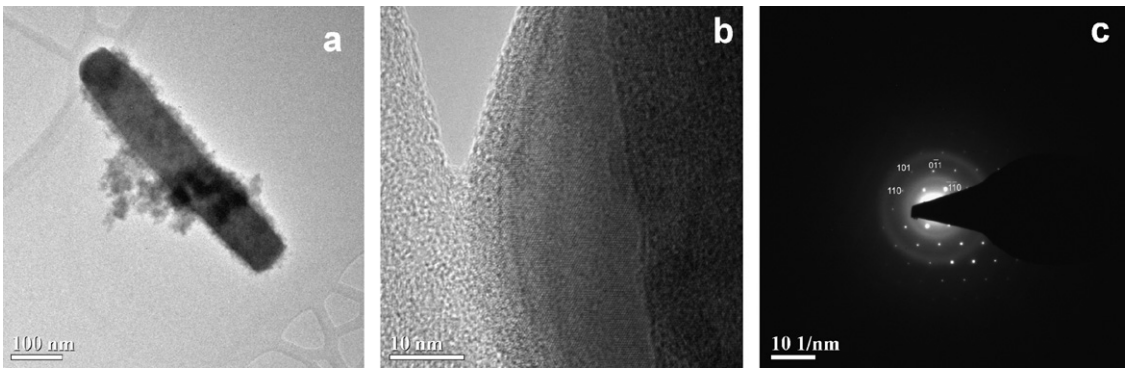

Fig. 3. (a) The TEM image of a SnO_2 nanorod on a holey-carbon TEM grid. (b) Enlarged HRTEM image of a single-crystalline SnO_2 nanorod and (c) the corresponding selected-area electron diffraction (SAED) pattern taken from a section of the nanorod.

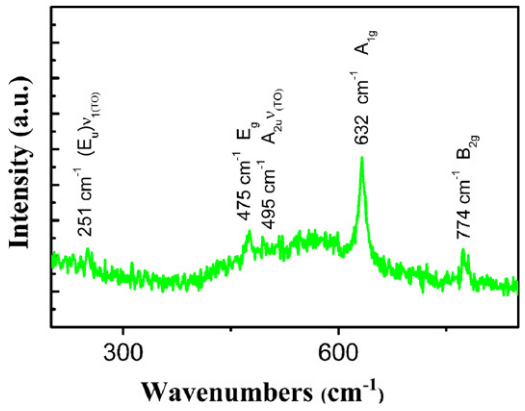

Fig. 4. Micro-Raman scattering spectra of the as-grown SnO_2 nanorods.

single crystal [17] and in agreement with data of group-theory analysis [18,19]. These peaks are attributed to the E_g, A_{1g}, and B_{2g} vibrational modes of SnO_2 [20].

SnO_2 with the rutile structure belongs to the space group P42/mnm and point group D_{4h} [21]. The $k = 0$ optical modes and their infrared (IR) and Raman (R) activity can be presented as follows [21]:

$$\Gamma = A_{1g}(R) + A_{2g}(F) + A_{2u}(IR, \|) + B_{1g}(R) + B_{2g}(R) + 2B_{1u}(F) + E_g(R) + 3E_u(IR, \perp) \quad (1)$$

Raman active modes are A_{1g}, B_{1g}, B_{2g}, and E_g, in these modes the oxygen atoms vibrate while the Sn atoms are at rest. The E_g mode represents vibrations in the direction of the c-axis, but A_{1g} and B_{1g} are modes describing vibrations perpendicular to the c-axis [21]. Seven modes of A_{2u} and $3E_u$ are IR active and two modes of A_{2g} and B_{1u} are inactive [22]. Fig. 4 shows the Raman spectra for A_{1g} mode which were broadened as the size of SnO_2 nanorods decreased [23]. The E_g, A_{1g}, and A_{2g} are depicted in the Raman scattering spectra and confirm the rutile structure of SnO_2 nanorods.

4. A proposed growth mechanism

Understanding of the growth mechanism of nanorods without the need in templates, surfactants or applied field is very important for the synthesis of new materials as well as for device applications.

A proposed growth mechanism of SnO_2 nanorods can be explained in terms of chemical reactions and crystal growth as follows. From the crystallization point of view, the synthesis of an oxide during of an aqueous solution reaction is expected to experience a hydrolysis-condensation (nucleation-growth) process.

In our experiments, we observe that the shape and aspect ratio of the as-prepared SnO_2 products is changed and decreases by varying the molar ratio of $SnCl_4$ to NH_4OH from 20:1 to 10:1, which is in agreement with the previous reports [11,24].

Growth of SnO_2 nanorods occurs according to the total reaction [11,24]:

$$Sn^{4+} + 4OH^- \rightarrow SnO_2 + 2H_2O \quad (2)$$

$$Sn^{4+} + 4OH^- \rightarrow Sn(OH)_4 \quad (3)$$

The amphoteric hydroxide $Sn(OH)_4$ dissolves in excess of ammonia solution and forms $[Sn(OH)_6]^{2-}$ anions:

$$Sn(OH)_4 + 2OH^- \rightarrow [Sn(OH)_6]^{2-} \quad (4)$$

During the hydrothermal reaction, the $[Sn(OH)_6]^{2-}$ ions decomposed into SnO_2:

$$[Sn(OH)_6]^{2-} \xrightarrow[\text{hydrothermal reaction}]{\text{kinetic growth regime}} SnO_2 + 2H_2O + 2OH^- \quad (5)$$

The appropriate molar ratio of Sn^{4+} to OH^- ions for the growth of SnO_2 nanorods is found to be 1:25–35. According to SEM images as presented in Fig. 2b, decreasing tin ions concentration to 0.02 M and below will produce quasi-spherical particles when all other conditions remain constant. By raising the concentration up to 0.015–0.02 M, nanorods will form. Change of the tin ion concentration in the reverse micelles is much higher than that in the bulk solution [25] and thus leads to morphology differences in agreement with previous reports [11,24]. It is also observed that increasing the temperature and extending the heating duration leads to an increase of the surface-to-volume ratio of nanorods. The concentration of tin ions in solution also influences to the size of nanorods.

The formation of SnO_2 nanorods was obtained with the progress of crystal growth. The kinetic growth regime during the hydrothermal reaction (Eq. (5)) is a decisive factor in the formation of tetragonal-shaped crystals. Here, has to be considered adjusting the concentration of precursors as described above, thus controlling the hydrolysis ratio and quality of the nuclei. Also, the hydrothermal temperature is an important factor affecting hydrolysis rate of SnO_2 nanorods growth. Thus, by regulating these parameters, the nucleation and growth processes directly on substrate can be controlled.

In our experiments, the hydrothermal process using described reaction media of aqueous metal–ion precursors allows a slow nucleation and growth at low-interfacial tension conditions, which favors the generation of tetragonal-shaped SnO_2 nanocrystals. In these conditions, the product morphology is dictated by the crystal symmetry as well as by the surface energy in aqueous environment and thus the most stable crystal habit is generated directly onto the substrates, without the need of surfactants or templates [12]. Also, the growth mechanism of SnO_2 nanorods can be explained on the base of its rutile structure, which is 6:3 coordinated and the bonding between atoms has a strong ionic character. The synthesized material is a square cross section nanocrystal (insert in Fig. 1) because of the tetragonal unit cell containing two tin atoms and four oxygen atoms. As was determined experimentally from our results, the tetragonal crystal growth is enclosed by the stable (110) facets, thus the rutile structure is built up from the neutral stacked layers of the following planes (O), (2Sn+O), and (O) with ionic charges 2−, 4+, and 2−, respectively, in the surface unit cell. In this way, it is possible that a termination with these planes of the SnO_2 (110) is called a stoichiometric surface. According to the presented results, SnO_2 can grow from solutions in well-defined tetragonal edges and giving a proper morphology.

Thus, by carefully adjusting of the balance between the thermodynamic and the kinetic growth regime, crystals can be formed with geometrical morphology consistent with its crystallographic structure. Also controlling the kinetic growth regime can promote the anisotropic growth along the high-energy crystallographic face. It is known that SnO_2 with rutile structure belongs to the (P42/mnm) space group with square pyramid as its thermodynamically stable crystallographic form [12]. According to theoretical studies—the (110) surface is the thermodynamically most stable termination [26] and has the lowest surface energy. It would therefore be expected to be predominantly in the nanomaterials morphology. At the same time the surface energy suggest that the (001) surface is very unstable. However, both planes (110 and 001) are close in attachment energies and can be

observed experimentally [12] and demonstrated theoretically [26,27].

5. Conclusion

SnO_2 nanorods were successfully grown directly onto SiO_2/Si substrates by a simple hydrothermal method. The SnO_2 nanorods are grown parallel to the [101] direction in the tetragonal rutile structure. The microstructures and surface compositions of the nanorods were characterized by XRD, TEM, SEM, and Raman spectra.

The results from Raman spectra and XRD patterns demonstrate that the obtained nanorods have the single crystalline rutile structure of SnO_2. The present process has the advantage of being very simple, its yields are high and the morphology of nanorods can be controlled.

Further work on optimization of the synthetic parameters such as heating temperature, duration, and rate to control the aspect ratio and different morphologies of the nanorods is underway in our laboratory.

Acknowledgments

L. Chow acknowledges financial support from Apollo Technologies, Inc. and the Florida High Tech Corridor Research Program. The research described here was made possible in part by an award for young researchers (O.L.) (MTFP-1014B Follow-on) from the Moldovan Research and Development Association (MRDA), under funding from the US Civilian Research & Development Foundation (CRDF). Raman measurements were supported in part by NSF MRI grant DMR-0421253.

References

[1] Z.W. Chen, J.K.L. Lai, C.H. Shek, Phys. Rev. B 70 (2004) 165314.
[2] Z. Dai, J.L. Gole, J.D. Stout, Z.L. Wang, Phys. Chem. B 106 (2002) 1274.
[3] G. Gao, Nanostruct. Nanomater., Imperial College Press, London, 2004.
[4] P. Yang, H. Yan, S. Mao, R. Russo, J. Johnson, R. Saykally, et al., Adv. Funct. Mater. 12 (2002) 719.
[5] O. Lupan, G. Chai, L. Chow, Microelectron. J. 38 (12) (2007) 1211.
[6] Y.J. Chen, X.Y. Xue, Y.G. Wang, T.H. Wang, Appl. Phys. Lett. 87 (2005) 233503.
[7] J.Q. Hu, X.L. Ma, Z.Y. Xie, N.B. Wong, C.S. Lee, S.T. Lee, J. Phys. Chem. B 106 (2002) 3823.
[8] Y. Liu, J. Dong, M. Liu, Adv. Mater. 16 (2004) 353.
[9] J.H. Ba, J. Polleux, M. Antonietti, M. Niederberger, Adv. Mater. 17 (2005) 2509.
[10] X.S. Peng, L.D. Zhang, G.W. Meng, Y.T. Tian, Y. Lin, B.Y. Geng, et al., J. Appl. Phys. 93 (2003) 1760.
[11] D.F. Zhang, L.D. Sun, J.L. Yin, C.H. Yan, Adv. Mater. 12 (2003) 1022.
[12] L. Vayssieres, M. Graetzel, Angew. Chem. Int. Ed. 43 (2004) 3666.
[13] O. Lupan, L. Chow, G. Chai, H. Heinrich, S. Park, A. Schulte, Growth of tetragonal SnO_2 microcubes and their characterization, Journal of Crystal Growth, doi:10.1016/j.jcrysgro.2008.10.072.
[14] O. Lupan, L. Chow, G. Chai, B. Roldan, A. Naitabdi, A. Schulte, Mater. Sci. Eng. B 145 (2007) 57.
[15] O.I. Lupan, S.T. Shishiyanu, L. Chow, T.S. Shishiyanu, Thin Solid Films 516 (2008) 3338.
[16] Joint Committee on Powder Diffraction Standards, Powder Diffraction File PDF# 021-1250.
[17] J.F. Scott, J. Chem. Phys. 53 (1970) 852.
[18] H. Kohno, T. Iwasaki, Y. Mita, S. Takeda, J. Appl. Phys. 91 (2002) 3232.
[19] V.G. Kravets, Opt. Spectrosc. 103 (2007) 766.
[20] P.S. Peercy, B. Morosin, Phys. Rev. B 7 (1973) 2779.
[21] R.S. Katiyars, P. Dawsons, M.M. Hargreaves, G.R. Wilkinson, J. Phys. C: Solid State Phys. 4 (1971) 2421.
[22] J.G. Traylor, H.G. Smith, R.M. Nicklow, M.K. Wilkinson, Phys. Rev. B 3 (1971) 3457.
[23] A. Dieguez, A. Romano-Rodriguez, A. Vila, J.R. Morante, J. Appl. Phys. 90 (2001) 1550.
[24] J. Zhang, L.D. Sun, J.L. Yin, H.L. Su, C.S. Liao, C.H. Yan, Chem. Mater. 14 (2002) 4172.
[25] M.P. Pileni, Langmuir 13 (1997) 3266.
[26] B. Slater, C. Richard, A. Catlow, D.H. Gay, D.E. Williams, V. Dusastre, J. Phys. Chem. B. 103 (1999) 10644.
[27] E.R. Leite, T.R. Giraldi, F.M. Pontes, E. Longo, Appl. Phys. Lett. 85 (2003) 1566.